  Bull. Chem. Soc. Jpn., 61, 379—383 (1988) 

# The Thermal Decomposition and Hydrolysis of Calcium Carbamoyl Phosphate

Choichiro SHIMASAKI* and Hiroki SUZUKI
Department of Industrial Chemistry, Faculty of Engineering, Toyama University, Gofuku, Toyama 930
(Received May 18, 1987)

Calcium carbamoyl phosphate (**1**) was prepared by adding an aqueous calcium chloride solution to a reaction solution of $KH_2PO_4$ with KOCN. **1** was unstable at room temprature. **1** was dehydrated to make anhydrous salt and thermally decomposed to liberate ammonia, cyanic acid, and carbon dioxide, finally resulting in the formation of calcium pyrophosphate in air. The apparent activation energies for the three endothermic peaks of the DTA curve were estimated to be 50.0, 83.9, and 148.3 kJ $mol^{-1}$ respectively. The hydrolysis of **1** in an aqueous solution apparently obeyed the first-order kinetics. The activation parameters for the hydrolysis of **1** were evaluated by using the $^{31}P$ NMR spectra of **1** with the lapse of the reaction time. The activation energy was 92.2 kJ $mol^{-1}$; the activation enthalpy, 89.7 kJ $mol^{-1}$, and the activation entropy, −6.3 e.u.

Some phosphor-nitrogen compounds are already used as industrial materials and obtained as industrial products. There are a series of phosphorus-nitrogen compounds which have amino groups on a P atom. There compounds have the potential for use as new flameproofing and glow-retardant agents on a large number of cellulosic materials; further, they can be used as the starting materials in the preparation of many organic and inorganic phosphorus compounds.

In our previous papers,[1-3] the thermal behavior of many phosphoramidates were reported. This paper will describe the synthesis, thermal behavior, and hydrolysis of calcium carbamoyl phosphate (**1**) containing nitrogen and carbon. This compound was instable even at room temperature, and its thermal product resulted in calcium pyrophosphate. It was found by $^{31}P$ NMR measurements that the hydrolysis of **1** apparently obeys the first-order kinetics.

## Experimental

**Preparation of Calcium Carbamoyl Phosphate.** **1** was synthesized by reference to the method described in the literature.[4] Potassium dihydrogenphosphate (0.1 mol) and potassium cyanate (0.1 mol) were dissolved in 100 $cm^3$ of water. To the resulting mixture, which had been cooled in an ice bath, two solutions of 60 ml of 1 mol $dm^{-3}$ $BaCl_2$ and 50 ml of 1 mol $dm^{-3}$ NaOH were slowly added, drop by drop with continuous stirring. During the treatment, the pH of the solution was kept at 9.0—9.3. The resulting cream-colored precipitate of barium monohydrogenphosphate was removed by suction filtration. The filtrate was transferred to a flask, and 50 ml of 1 mol $dm^{-3}$ $CaCl_2$ was added, drop by drop. To the resulting solution was slowly added 100 ml of ethanol. The resulting white precipitate was collected by suction filtration, washed with several small portions of water, ethanol, and acetone, air-dried, and finally dried in a vacuum over diphosphorus pentaoxide for 48 h.

**Chemical Analysis.** The phosphorus in a sample was determined colorimetrically by the molybdenum-blue method. The calcium in a sample was estimated by the atomic-absorption-analysis technique. The nitrogen, carbon, and hydrogen in a sample were determined by using a Hitachi C, H, N analyser-026 at the Toyama Medical and Pharmacy University.

**Measurements.** The thermal analysis measurements were made in air by using a Rigakudenki TG-DTA, DSC apparatus, at the heating rates of 3, 5, 6, 8, and 10 K $min^{-1}$ for TG-DTA and 5 K min for DSC respectively. The IR spectra of the sample were recorded on a Nipponbunko IR-810 apparatus using the KBr-disc method. For the $^{31}P$ NMR spectra, a sample of about 100 mg was put in 5.0 $cm^3$ of a 6% EDTA deuterated-water solution and stirred for several minutes. A JNM-FX 90 Fourier transform spektrometer was used to measure the $^{31}P$ NMR spectra. An X-ray diffraction diagram of a powder sample was taken with nickel-filtered Cu $K\alpha$ radiation using a Shimazu X-ray diffractometer XD-5, XD-3A, and a Rigaku RAD-RVB apparatus.

## Results and Discussion

**Thermal Behavior.** The DTA and TG curves of **1** are shown in Fig. 1. The DTA curve indicated four endothermic peaks in this range: r.t.—362, 362—430, 430—465, and 465—541 K, while the TG curve indicated a slow decrease in the weight. For each type of peak ($E_{D1}$, $E_{D2}$, $E_{D3}$, and $E_{D4}$) shown in Fig. 1, two temperatures are recorded; the first one is the point of departure from the base line, while the second one is the end point of the peak temperature. The indication of "temperature" on the DTA curve in Fig. 1 means the temperature at which samples were removed from a furnace prior to being cooled in a silicagel desiccator and subjected to further research. The results of the elemental analyses of the thermal products are shown in Table 1. It can be seen from Table 1 that the nitrogen, carbon, and hydrogen contents of the thermal product decreased in the heating process and that the

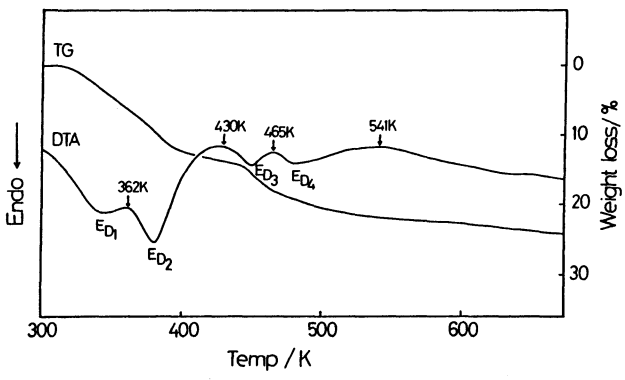


Fig. 1. DTA and TG curves of $CaCAP \cdot 1.5H_2O$. Heating rate: 5 K $min^{-1}$.

thermal product at 541 K contained no nitrogen and hydrogen. These data on the reduction in weight after 30 min at each endothermic peak temperature were not always in agreement with those calculated from the TG curve. The results showed that carbon dioxide, ammonia, and cyanic acid are exhausted in the case of the thermal condensation of **1**.

The IR spectra of the thermal products are shown in Fig. 2. For the IR spectrum of **1**, the absorption band at about 3400 $cm^{-1}$ is assigned to the N-H stretching vibration; those at 1680 and 1730 $cm^{-1}$, to the C=O stretching vibration; those at 1610 and 1630 $cm^{-1}$, to the N-H deformation vibration; that at 1400 $cm^{-1}$, to the C-N stretching vibration; that at 1150 $cm^{-1}$, to the P=O stretching vibration; that at 980 $cm^{-1}$, to the P-O-C stretching vibration, and that at 570 $cm^{-1}$, to the $(PO_2)^-$ or $(PO_3)^{2-}$ deformation vibration. These absorptions grew weaker with an increase in the temperature, and they disappeared in the thermal product at 430 K. At about 910 $cm^{-1}$, the absorption band attributed to the P-O-P antisymmetric stretching vibration grew strong. This showed that the condensation polymerization was proceeding. For the thermal product at 362—673 K, the absorption band of carbon dioxide was observed at 2350 $cm^{-1}$. Also, for the thermal product at 1073 K, the absorption observed at 900—1250 $cm^{-1}$ was very complex, with strong peaks. This complexity of absorption was attributed to the progress of the crystallization.

Table 1. Elemental Analysis of the Thermal Products of $CaCAP \cdot 1.5H_2O$

| Sample | Ca/% | P.% | N/% | C/% | H/% |
|---|---|---|---|---|---|
| r.t.[a] | 19.1 | 15.0 | 6.2 | 5.4 | 2.3 |
| | (19.4) | (15.0) | (6.8) | (5.8) | (2.5) |
| 362 K | 21.5 | 16.1 | 5.4 | 5.1 | 2.1 |
| 430 K | 25.2 | 19.3 | 3.4 | 3.1 | 1.3 |
| 465 K | 25.4 | 20.9 | 2.1 | 2.9 | 0.5 |
| 541 K | 27.2 | 21.7 | 0.0 | 2.1 | 0.0 |
| 673 K | 30.1 | 23.7 | 0.0 | 1.6 | 0.0 |
| 1273 K[b] | 32.5 | 24.5 | 0.0 | 0.0 | 0.0 |
| | (32.8) | (25.4) | | | |

a) Calculated values in parentheses as $CaCAP \cdot 1.5H_2O$.
b) Calculated values in parentheses as $Ca_2P_2O_7$.

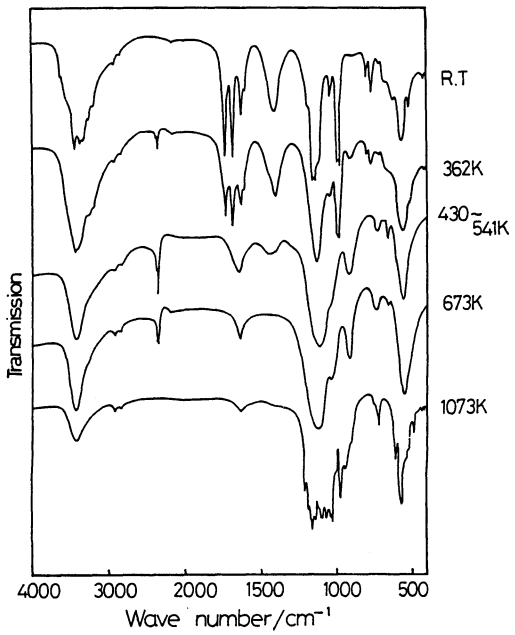


Fig. 2. IR spectra of the thermal products of $CaCAP \cdot 1.5H_2O$.

The $^{31}P$ NMR spectra of the thermal products are shown in Fig. 3. As has been mentioned previously, **1** is very instable at room temperature; therfore, the

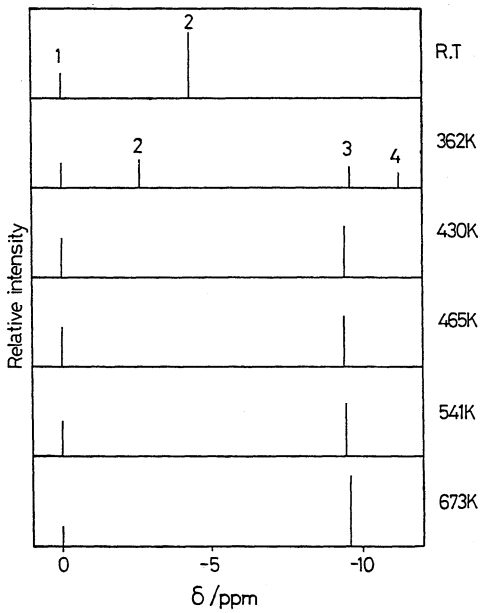


Fig. 3. $^{31}P$ NMR spectra of the thermal products of $CaCAP \cdot 1.5H_2O$. 1: Orthophosphate, 2: carbamoylphosphate, 3: diphosphate, 4: end $PO_4$ group of intermediate polyphosphate ($n>3$).

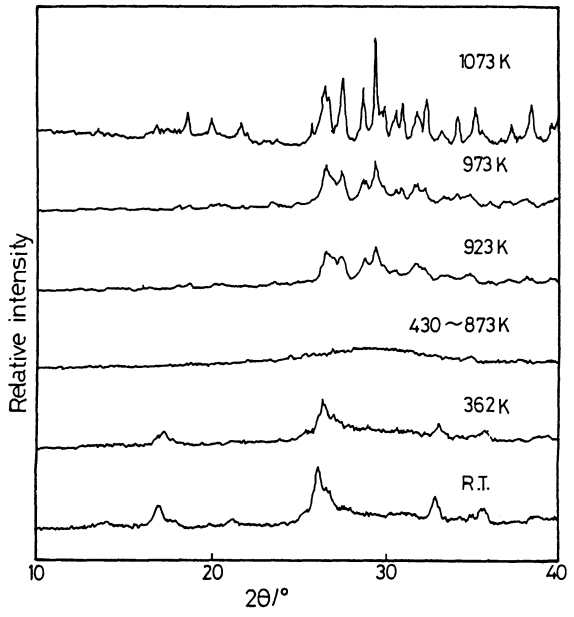


Fig. 4. X-Ray diffraction diagrams of the thermal products of $CaCAP \cdot 1.5H_2O$. Heating rate: 2 K $min^{-1}$.

$^{31}P$ NMR spectrum of **1** indicated peaks caused by a carbamoyl phosphate (CAP) and an orthophosphate ($PO_4$). The molar ratio CAP/(CAP+$PO_4$), is calculated by means of the signal area, was 0.88 for **1**. The $^{31}P$ NMR spectrum of the thermal product at 362 K indicated peaks attributable to a $PO_4$, a CAP, a diphosphate ($P_2O_7$), and an intermediate of the thermal condensation. The thermal product at 430 K indicated no CAP peak, but peaks of $PO_4$ and $P_2O_7$ were both registered. These results agreed with those of the IR spectra. The peak of $P_2O_7$ grew stronger above 430 K.

The X-ray diffractions of the thermal product at a given isothermal temperature, as obtained by using XD-3A, are shown in Fig. 4. No diffraction patterns on the thermal products were observed at room temperature at 430—873 K. The X-ray diffraction of the thermal product at 973 K indicated weak patterns, but these patterns were much clearer than those at 923 K. The X-ray diffraction patterns of the thermal products at the temperature interval from 465 to 673 K, as obtained using the Rigaku RAD-RVB apparatus, were similar to the amorphous solid compositions, as is shown in Fig. 4. The thermal product at 1073 K showed strong X-ray diffraction patterns of $\alpha$-$Ca_2P_2O_7$.[5]

**Decomposition at Room Temperature.** The stability of **1** was checked at room temperatue (283—303 K) in air. Figure 5 should the IR and $^{31}P$ NMR spectra of the decomposition of **1** at room temperature. **1** was very instable at room temperature. At 910 $cm^{-1}$, the absorption of the P-O-P antisymmetric stretching vibration appeared, and its intensity increased with the lapse of the reaction time. Therefore, either the polymerization or the condensation of **1** seemed to be progressing. This agrees with the results of the IR and $^{31}P$ NMR spectra. A peak attributable to $P_2O_7$ appeared after the lapse of 8 dyas, and its intensity increased with the lapse of the reaction time. A peak due to CAP decreased with the lapse of the reaction time. A peak due to CAP decreased with the lapse of the reaction time, on the other hand, and disappeared at 133 days.

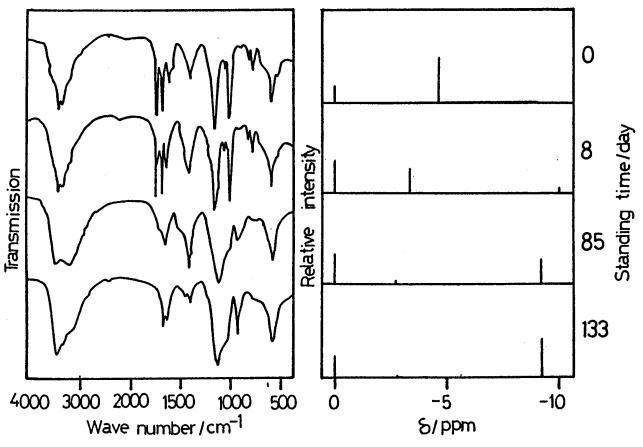


Fig. 5. IR and $^{31}P$ NMR spectra of the decomposition of CaCAP·1.5$H_2O$ at room temperature.

**Kinetic Studies of Thermal Process.** Kinetic studies of the pyrolysis (i.e., dehydration and condensation) of **1** were done by the Kissinger method[6] on the basis of the DTA peaks $E_{D1}$—$E_{D4}$, as is shown in Fig. 1. As the heating rate increased, both the initial transition and the peak maximum for dehydration and condensation were shifted to higher temperatures. The theoretical work of Kissinger indicated that the activation energy of the pyrolysis process of **1** was defined by the following form:

$$\frac{d \ln (\phi/T_m^2)}{d(1/T_m)} = -E/R$$

where $\phi$ stands for the heating rate; $T_m$, for the temperature of the DTA-maximum, $E$, for the activation energy, and $R$, for the gas constant. These plots of $\ln(\phi/T_m^2)$ against $1/T_m$ are linear, the slop being equal to $-E/R$. Thus, the apparent activation energies of each pyrolysis process were obtained from this slop. The apparent activation energies for the three endothermic peaks (=$E_{D1}$, $E_{D2}$, and $E_{D3}$) were estimated to be 50.0, 83.9, and 148.3 kJ $mol^{-1}$ respectively. The results are shown in Fig. 6 and Table 2. As the heating rate increased, the peak maximum for $E_{D4}$ was not appreciably shifted. It was found that the $E_{D4}$ peak was caused by the heat of crystallization.

According to these results, the pyrolysis mechanism of **1** may be written as Scheme 1. **1** is dehydrated to

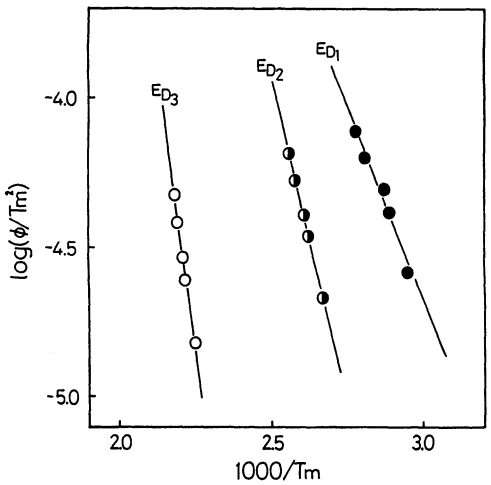


Fig. 6. The Kissinger's plots for $E_{D1}$, $E_{D2}$, and $E_{D3}$ in DTA curves for CaCAP·1.5$H_2O$.

Table 2. Kinetic Data for the Pyrolysis of CaCAP·1.5$H_2O$

| DTA peak | Equation of straight line | $r^{a)}$ | $E$/kJ·mol$^{-1}$ |
|---|---|---|---|
| $E_{D1}$ | $\log(\phi/T_m^2)=-2.609\cdot1000/T_m+3.147$ | 0.985 | 50.0 |
| $E_{D2}$ | $\log(\phi/T_m^2)=-4.378\cdot1000/T_m+7.019$ | 0.996 | 83.9 |
| $E_{D3}$ | $\log(\phi/T_m^2)=-7.735\cdot1000/T_m+12.550$ | 0.999 | 148.3 |

a) Linear correlation coefficient.

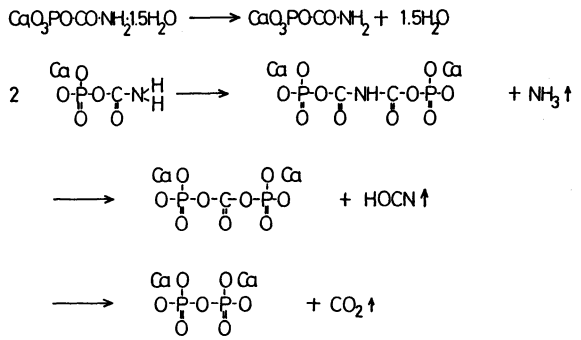

Scheme 1.

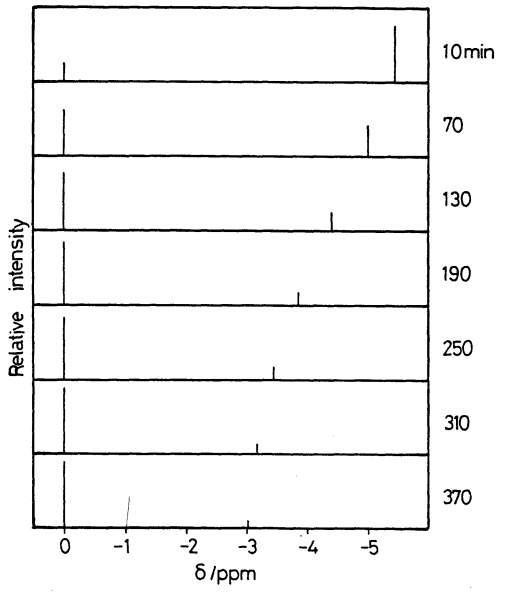


Fig. 7. $^{31}$P NMR spectra of CaCAP·1.5H$_2$O with the elapse of the reaction time at 302.6 K.

make anhydrous salts. Next, the anhydrous salts are bimolecularly condensed to liberate ammonia, cyanic acid, and carbon dioxide. Finally, calcium pyrophosphate is formed.

**Hydrolysis of Calcium Carbamoyl Phosphate in an Aqueous Solution.** The hydrolysis of **1** in an aqueous solution seems to progress as follows:

$$OPO_3 \cdot CO \cdot NH_2^{2-} + H_2O \rightarrow PO_4H_2^- + CO_2NH_2^-,$$
$$CO_2NH_2^- + PO_4H_2^- + H_2O \rightarrow CO_3H^- + NH_4^+ + PO_4H^{2-}.$$

$^{31}$P NMR measurement was used to investigate the hydrolysis reaction of **1** at temperatures from 299.0 to 315.2 K. The $^{31}$P NMR spectra of **1** with the lapse of the reaction time at 302.6 K are shown in Fig. 7. These spectra indicated peaks attributable to CAP and $PO_4$; the former decreased and shifted to a low magnetic field with the lapse of the reaction time. The chemical shifts of the $^{31}$P NMR spectra at various temperatures, taken at intervals, are shown in Fig. 3. Smooth curves were obtained at all temperatures. The speed of shifting grew rapidly with the rise in the temperature. After the lapse of an infinite time, the peak due to CAP was shifted by about −2.6 ppm. This phenomenon is independent of the pH, as was shown in the pH measurement of a solution[7] with the lapse of the reaction time over a period of 307 min. As Fig. 7 shows, the peak attributable to CAP decreased and that attributable to $PO_4$ increased with the lapse of the reaction time (apparently obeying the first-order kinetics). The first-order kinetics can represented as follows:

$$kt = \ln \frac{a_0 - a_\infty}{a_t - a_\infty},$$

where $a_0$ and $a_\infty$ are the CAP/(CAP+$PO_4$) molar ratios at the beginning and when the reaction is complete respectively; $a_t$, the value after time $t$, and $k$, the rate constant. $a_0$, $a_\infty$, and $a_t$ were determined by measuring the integral intensities of the $^{31}$P NMR spectrum for CAP and $PO_4$ respectively. The first-order kinetic

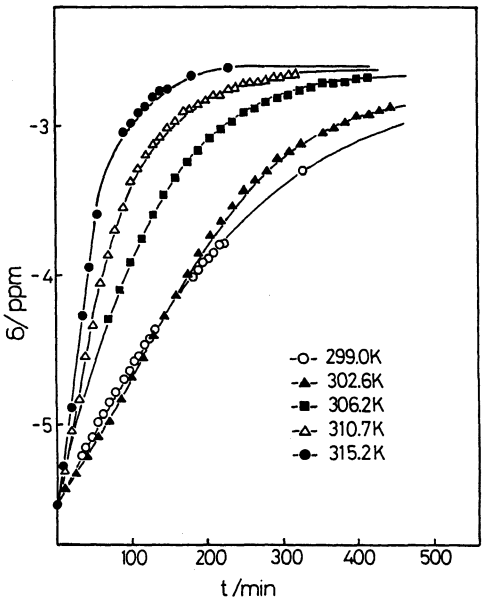


Fig. 8. The chemical shift of $^{31}$P NMR spectra at various temperatures.

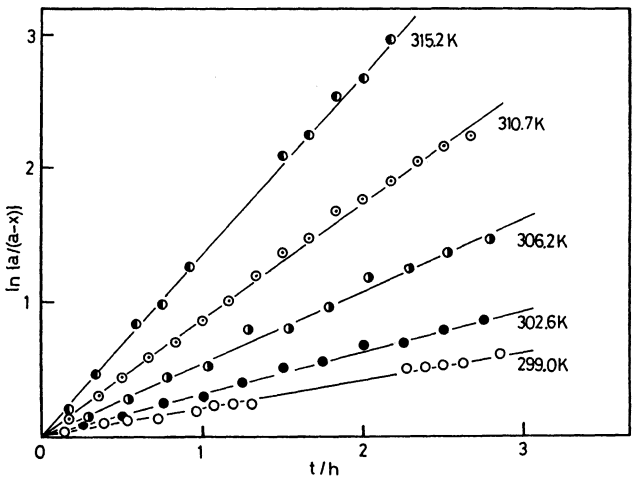


Fig. 9. The first order kinetic plots of ln $a/(a-x)$ vs. $t$ for the hydrolysis of CaCAP·1.5H$_2$O in aqueous solution.

plots of $\ln[(a_0-a_\infty)/(a_t-a_\infty)]$ vs. $t$ at various temperatures were found to be linear, as is shown in Fig. 9. The rate constants for the hydrolysis of **1** are shown in Table 3. Arrhenius plots (Fig. 10) give us the activation energy and the frequency factor. The activation enthalpy and entropy were obtained by using the values of the activation energy and the frequency factor. These kinetic data are tabulated in Table 4.

One of the most significant treatments of the theory of reaction rates is based on the concept of the existence of an activated complex as an intermediate stage in all chemical reactions. In a reaction involving two or more molecules, the reactants, possessing sufficient energy, must approach one another closely. Since in any bimolecular reaction except in the dissociation of two molecules, a reaction with $A \doteqdot 10^{11}\,M^{-1}\cdot s^{-1}$ is generally regarded as a standard bimolecular reaction,[8] the value of the frequency factor in this paper suggests a bimolecular reaction. Even in a unimolecular reaction, in which a single molecule takes part in each chemical act, it is necessary for some rearrangement of atoms and energy to occur, thus giving the requisite activated complex, before a reaction can take place. From the results of Table 4, the value of the activation energy can be said to be approximately identical to that of the activation enthalpy. By supposing that an equilibrium exists between the reacting molecules and the activated complex, which decompose at a definite rate, it has been found possible to estimate the apparent $\Delta S^*$ value for the hydrolysis reaction. Such a $\Delta S^*$ value suggests that mechanism of the hydrolysis reaction consists of two main complicating steps which can be described by the above chemical equations.

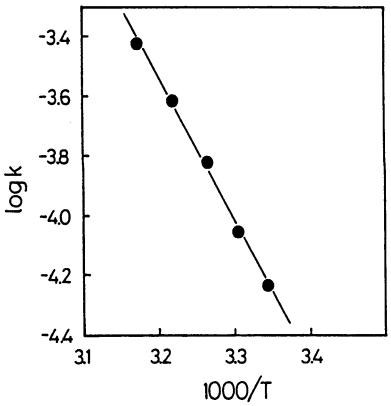


Fig. 10. Arrehenius plots of the first order rate constants for the hydrolysis of CaCAP·1.5$H_2O$ in aqueous solution.

Table 3. Rate Constants for the Hydrolysis of CaCAP·1.5$H_2O$ in an Aqueous Solution

| $T$/K | Rate constant $k/s^{-1}$ | $r^{a)}$ |
|---|---|---|
| 299.0 | $5.82\times10^{-5}$ | 0.997 |
| 302.6 | $8.83\times10^{-5}$ | 0.998 |
| 306.2 | $1.51\times10^{-4}$ | 0.996 |
| 310.7 | $2.42\times10^{-4}$ | 0.999 |
| 315.2 | $3.78\times10^{-4}$ | 0.999 |

a) Linear correlation coefficient.

Table 4. Kinetic Data for the Hydrolysis of CaCAP·1.5$H_2O$ in an Aqueous Solution

| $A/s^{-1}\,mol^{-1}$ | $E_a$/kJ mol$^{-1}$ | $\Delta H^*$/kJ mol$^{-1}$ | $\Delta S^*$/e.u. |
|---|---|---|---|
| $7.02\times10^{11}$ | 92.2 | 89.7 | −6.3 |

We wish to thank Professor Ikuya Matsuura and Mr. Akira Matsui for the X-ray diffraction analysis, Mr. Kiyoshi Terayama for the DTA-TG, and Mr. Yoshiharu Yoneyama for the NMR spectra.

**References**

1) C. Shimasaki, Y. Oono, F. Takai, M. Shoji, and M. Yoshizawa, *Nippon Kagaku Kaishi*, **1982**, 376.

2) C. Shimasaki, S. Ookawa, and R. Ishizaka, *Bull. Chem. Soc. Jpn.*, **58**, 592 (1985).

3) C. Shimasaki and M. Hara, *Bull. Chem. Soc. Jpn.*, **58**, 3613 (1985).

4) F. Seel and F. Schineeling, *Z. Naturforsch.* **33b**, 374 (1978).

5) "Index (inorganic) to the powder diffraction file," American Society for Testing Materials (1968). Jcpds Cards 9-345.

6) H. E.Kissinger, *Anal. Chem.*, **29**, 1702 (1957).

7) CaCAP 1.5$H_2O$ (0.4 g) was dissolved in 50 ml of a 6% EDTA deuterated-water solution.

8) T. Fueno, "Kagaku Hannoron," Asakura, Tokyo (1975), p. 123.